HYDROLOGICAL PROCESSES
Hydrol. Process. **16**, 3079–3089 (2002)
Published online 17 September 2002 in Wiley InterScience (www.interscience.wiley.com). DOI: 10.1002/hyp.1090

Improved method for modelling sediment transport on unpaved roads using KINEROS2 and dynamic erodibility

Alan D. Ziegler,[1,2]* Thomas W. Giambelluca[2] and Ross A. Sutherland[2]
[1] *Environmental Engineering and Water Resources, Princeton University, Princeton NJ 08544*
[2] *Department of Geography, University of Hawaii, 2424 Maile Way 445, Honolulu HI 96822*

Abstract:

One difficulty in modelling sediment transport on unpaved road surfaces stems from the inability of physically based models to simulate the flush of loose surface material that is deposited on the road surface prior to the onset of a storm. This work builds upon a prior modelling methodology (referred to as dynamic erodibility) to simulate time-varying sediment transport on unpaved mountain roads by loosely coupling a continuous, exponential decay disturbance model with the erosion algorithm in KINEROS2. The method is tested against sediment transport time-series observed on small-scale rainfall simulation plots for various slope, antecedent soil wetness and pre-storm sediment availability conditions. The new method generally improves prediction errors of total sediment output, peak sediment output and fit of the sediment output time-series. However, for some validation events, the method fails to simulate high initial sediment spikes. This limitation may be a side-effect of using data from small-scale plots, but also may signify the need for additional calibration of the disturbance model subcomponent with data from surfaces having a greater variety of pre-event surface material. Nevertheless, this road erosion modelling approach provides a realistic 'description' of time-varying sediment transport, which is controlled both by the baseline erodibility of the underlying road surface, and importantly, by the removal of a loose, surficial sediment layer by overland flow. Copyright © 2002 John Wiley & Sons, Ltd.

KEY WORDS road erosion modelling; process geomorphology; sediment transport; watershed management

INTRODUCTION

The Thailand Roads Project was initiated in 1997 to determine the role of roads in initiating hydrological change and contributing to erosion processes in mountainous tropical watersheds. Current efforts in the Pang Khum Experimental Watershed (PKEW) in northern Thailand (Figure 1) are directed toward quantifying sediment inputs to the stream network from roads and other human-impacted lands, particularly steep agricultural fields. Our preliminary fieldwork suggests that PKEW roads may be on the same order of importance as agricultural lands in contributing to basin sediment flux, despite occupying a fraction of the land surface area. To assist in investigating the impacts of roads versus agriculture, it is desirable to develop a physically based modelling approach to simulate realistically road erosion processes. In a prior work (Ziegler *et al*., 2001a) we explored modelling road erosion using the KINEROS2 model (Smith *et al*., 1995, 1999). Data from three suites of rainfall simulation experiments were used to parameterize KINEROS2 for predicting runoff and sediment transport observed on small-scale (3·0–3·7 m^2) road plots, varying in slope, antecedent soil moisture and sediment availability. Results from this modelling endeavor include the following:

* Correspondence to: Alan D. Ziegler, Princeton University, Environmental Engineering and Water Resources, Water Resources Program, CEE E-Quad E-228 Princeton, NJ 08544, USA. E-mail: adz@princeton.edu

Received 13 November 2000
Accepted 14 December 2001

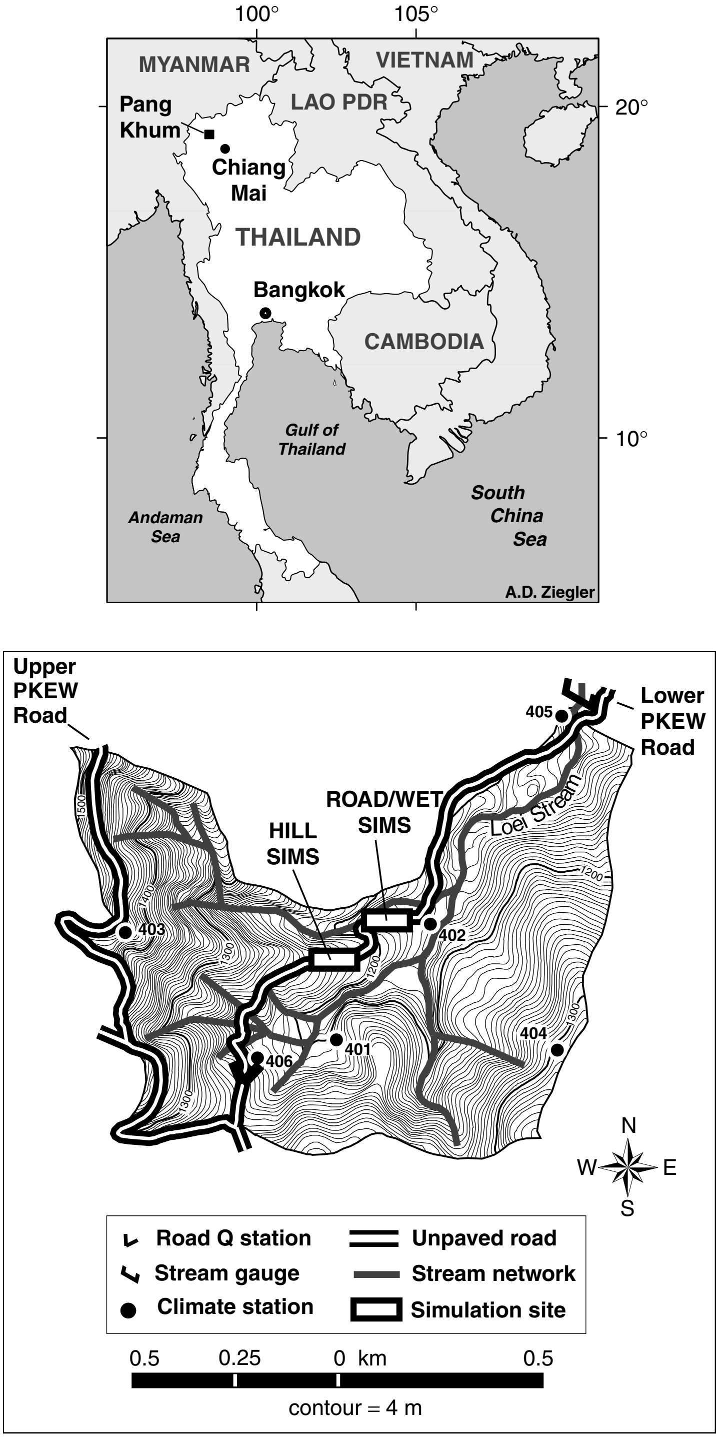

Figure 1. The Pang Khum Experimental Watershed in northern Thailand. Rainfall simulations were performed on the 1650-m main road within the watershed

1. Under all experimental conditions, KINEROS2 modelled runoff response realistically, both in terms of predicting total runoff and the instantaneous discharge (Q_t) times-series (e.g. Figure 2a and b).
2. KINEROS2 predicted total sediment output with little error (Table I), but failed to simulate typical sediment transport response (S_t) on the unpaved PKEW roads (dotted line, Figure 2c and d). This response (open circles in Figure 2c and d) is characterized by an initial flush of loose surface material, followed by a rapid decline in output as the volume of loose material is depleted, then a gradual decrease as sediment transport becomes controlled by the erodibility of the compacted road surface.
3. Prediction of the sediment transport times-series was improved by explicitly modelling the flush of loose surface sediment (solid line, Figure 2c and d). This was accomplished by allowing road surface erodibility to change during the course of a modelled storm; we refer to this modelling treatment as dynamic erodibility (DE, also see Ziegler *et al*., 2000a).

In the prior modelling effort, DE was implemented using a step function that determines changing erodibility states over the course of a storm (depicted in Figure 3). Initial erodibility (E_n) is a function of pre-storm sediment availability. In Figure 3, E_0 represents the 'baseline' erodibility of the underlying composite road surface, without the presence of a loose surface sediment layer. Intermediate erodibility states are reached as defined percentages of the loose material are removed; these percentages were assigned based on rainfall simulation data. In this work, we improve the original DE methodology by replacing the step function with a disturbed surface erosion model (continuous exponential decay function) that can simulate the initial flush and subsequent decline in the sediment transport time series.

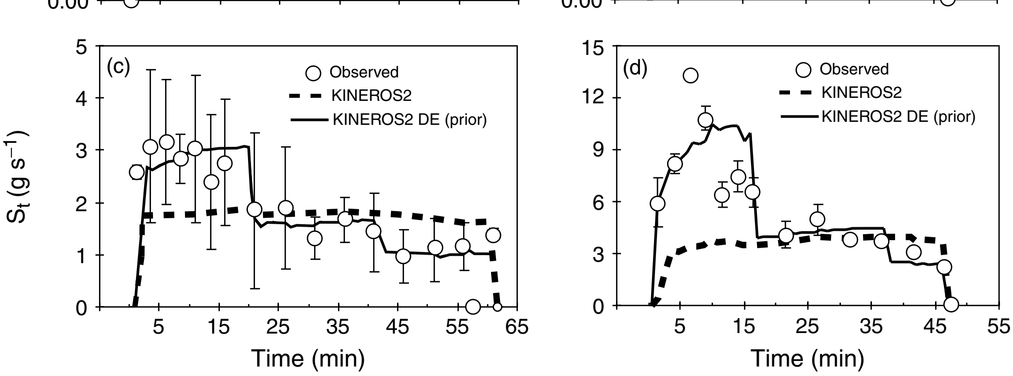

Figure 2. Comparison of discharge (Q_t) and sediment transport (S_t) data observed during ROAD and HILL rainfall simulation experiments (open circles) with that predicted using the standard KINEROS2 modelling functionality and by utilizing the dynamic erodibility (DE) method introduced in a prior work (Ziegler *et al*., 2001a). For both strategies Q_t is the same. Observed data are medians of the experiments indicated in the title (i.e., ROAD12457 refers to ROAD events 1, 2, 4, 5 and 7; HILL is the median of four events); error bars are ± one median absolute deviation about the median

Table I. Model calibration results, including errors and performance statistics, for KINEROS2-predicted sediment output using the standard model approach (STD), the dynamic erodibility method in the prior study (DE prior), and the technique introduced in this study (DE)

Simulation identity	Observed (kg)	Predicted (kg)	E_{total}[a] (%)	E_{peak} (%)	RMSE (%)
ROAD12457 STD	6·2	6·2	0	−41	52
ROAD12457 DE (prior)	6·2	6·5	4	−4	35
ROAD12457 DE	6·2	5·9	−5	0	15
HILL STD	15·7	10·7	−32	−67	70
HILL DE (prior)	15·7	14·6	−7	−22	45
HILL DE	15·7	16·5	5	−4	39

[a] E_{total} is error in total output estimate; E_{peak} is error in peak estimate; RMSE is root mean square error.

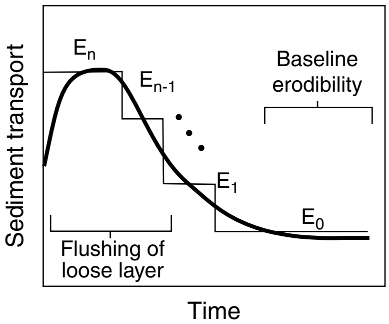

Figure 3. Characteristic sediment transport response on unpaved roads during constant rainfall, during which rut incision does not occur (thick line). The decline in sediment transport, as loose surface material is removed from the road, was modelled in a prior work (Ziegler *et al*., 2001a) by allowing road surface erodibility (values of *E*) to change throughout an event via a step function (thin line)

STUDY AREA

The PKEW is part of the larger Rim River Basin that eventually drains into the Ping River, which empties into the Chao Praya River. Bedrock in the PKEW is Triassic granite; soils include Ultisols, Alfisols and Inceptisols (field survey). Roads, access paths and dwelling sites comprise about 1% of the PKEW area. Based on 1995 aerial photographs and recent ground cover surveys, approximately 12% of the basin area is active agricultural land; 13% is fallow land; 31 and 12% are young (4–10 years) and advanced (>10 years) secondary vegetation, respectively; and 31% is disturbed, old-growth forest. Many of lower slopes in the basin are cultivated by Lisu villagers who migrated to Pang Khum from Mae Hong Son Province 20–25 years ago. The farming system now resembles a long-term cultivation system with short fallow periods, as opposed to the traditional Lisu long-fallow system (cf. Schmidt-Vogt, 1998). Owing to low saturated hydraulic conductivity and the high connectivity of the road network, the PKEW roads are capable of contributing disproportionately to basin runoff hydrographs (Ziegler and Giambelluca, 1997). Approximately 70% of all road runoff in PKEW directly enters the stream network at intersections of the road and stream channel. Despite light traffic and maintenance, the Upper and Lower PKEW Roads are important sediment sources for material entering the stream channel network each rainy season. Preliminary data suggest roads may be on the same level of importance as the agricultural practices in contributing to stream sedimentation and disrupting storm flow response in the basin (discussed in Ziegler *et al*., 2000a; 2001c).

METHODS

KINERSOS2

KINEROS2 is an event-based, quasi-physics-based model that simulates excess-infiltration runoff and erosion (Smith *et al*., 1995, 1999). Dynamic, distributed flow modelling in KINEROS2 is well-suited to simulate road runoff and erosion processes in the PKEW, where runoff generation on unpaved roads is dominated by the Horton overland flow (HOF) mechanism. Net erosion rate (e_{net}) in KINEROS2 is represented as the sum of rainsplash (e_s) and net hydraulic erosion (e_h) subcomponents (Smith *et al*., 1999)

$$e_{net} = e_s + e_h \tag{1}$$

Splash erosion is estimated from the relation

$$e_s = SPL(1 - \gamma)\exp(-c_d\overline{h})r^2 \tag{2}$$

where r is rainfall intensity, γ is the fraction of covered soil, $\overline{h}$ is depth of surface runoff, c_d represents the effect of water depth in damping rainsplash detachment (i.e. the exponential function reduces splash detachment as water depth increases) and the *SPL* parameter represents the *susceptibility* of the soil surface to rainsplash detachment. Flow-induced net hydraulic erosion is calculated as a function of current local sediment concentration (C_s) and transport capacity (C_m)

$$e_h = CH\, v_s(C_m - C_s) \tag{3}$$

where v_s is settling velocity and *CH* is a parameter that determines soil entrainment by flowing water (e.g. it is often inversely related to the soil cohesion). KINEROS2 is explained further by Smith *et al*. (1999). The reader will notice a slight variation in our present description of the model equations from that in the prior work; this reflects recent advances to KINEROS2 and its current description by the model developers (Carl Unkrich, USDA–ARS, Tuscon, AZ, personal communication).

Disturbed surface erosion model

Herein we loosely couple the sediment transport algorithm in KINEROS2 to an empirical exponential decay function to simulate the typical sediment transport response described in Figure 3. The decay function is based on the sediment-supply model used by Megahan (1974) to describe declines in sediment transport on unpaved roads over time following 'disturbance', such as road construction. For any site, Megahan's model is expressed as

$$\varepsilon_n = \varepsilon_0 + k\, S_n \exp(-kt) \tag{4}$$

where ε_n represents the erosion rate at a disturbed site, ε_0 is the erosion rate of the site prior to disturbance (i.e. the baseline erosion rate of the road surface), k, which occurs twice, represents the recovery potential for the disturbed site and t is time. The term S_n is an index of the amount of material made available by the disturbance.

Whereas the original model was based on seasonal data, we implement it for individual storm events. For example, we represent S_n as a power function of pre-storm surface sediment availability (d_n, kg m^{-2})

$$S_n = d_n^{\beta} \tag{5}$$

We also replace time in the exponential function with cumulative storm discharge (q, m), and add a shape (λ) parameter to the second term. The resulting model is

$$\varepsilon_n = \varepsilon_0 + \lambda k d_n^{\beta} \exp(-kq) \tag{6}$$

where values for λ, k and β are determined during parameter calibration/optimization using observed rainfall simulation data (described below). To accomplish DE modelling, ε_0 is simply the KINEROS2-predicted sediment transport value for the baseline erosion condition at each model time-step; and the second term, which is driven by KINEROS2-predicted discharge, produces the flush of the loose surficial sediment layer.

Rainfall simulation experiments in the PKEW

Three suites of 90–120 mm h^{-1} rainfall simulation experiments were used to provide data for calibrating and testing the new DE modelling approach. These experiments cover the range of slope, antecedent soil wetness and sediment availability conditions found in the PKEW throughout the course of a typical wet season. The experiments, which are described in detail elsewhere (Ziegler *et al.*, 2001b), are summarized as follows:

1. Eight, 60-min *ROAD* experiments were performed before the initiation of the wet season. We assume that these surfaces represent the PKEW roads following a lengthy dry period, during which vehicle traffic has detached an ample layer of loose surface material. Mean slope of the ROAD plots was 0·14 m m^{-1}; available loose surface material, d_n, was 1·8 kg m^{-2}(d_n values were determined from cross-sectional measurements, described in Ziegler *et al.*, 2001a).
2. Four *HILL* experiments were performed on a steeper (0·26 m m^{-1}) road section during the same dry period as the ROAD simulations. Owing to greater sediment detachment by vehicles ascending and descending the relatively steep hill section, the HILL plots contained approximately three times more loose surface material ($d_n = 5{\cdot}4$ kg m^{-2}) than the ROAD experiment plots. The HILL plots also are probably representative of heavily used road sections in the PKEW, regardless of slope.
3. Eight *WET* experiments were conducted on the ROAD simulation plots approximately 18 h following the conclusion of those simulations. The closeness (in time) of the ROAD and WET simulations ensured that the test surface was both relatively wet (0·22 versus 0·12 g g^{-1}) and free of loose surface material ($d_n \approx 0{\cdot}20$ kg m^{-2}); the latter was removed during the preceding ROAD rainfall simulation. We therefore assume that the WET plots represent a typical wet-season road surface, on which most loose surface material has been removed during prior runoff events.

Testing of the disturbance model

We calibrate the dynamic erodibility methodology by assigning KINEROS2 parameters SPL, CH and Manning's n values that allow the model to simulate the baseline erodibility of the PKEW road surface (i.e. E_0 in Figure 3). To do so, we use the values determined in the prior modelling work (139·95, 0·0105 and 0·015, respectively). The terms λ, k and β in the disturbance model are determined using an optimization algorithm that fits Equation (6) simultaneously through sediment transport data observed during the ROAD12457 (i.e. median values from ROAD events 1, 2, 4, 5 and 7) and HILL (median values from four events) rainfall simulation experiments. Slope and d_n values used are those described in the summary immediately above; other KINEROS2 parameters used herein are identical to those used in the prior work (Ziegler *et al.*, 2001a). During optimization we minimize the error in peak output and fit of the S_t time-series (as indicated by the root mean square error, RMSE); we meanwhile restrict the total error (E_{total}) in predicted sediment transport to be $\leq$5%. The three measures of model error or performance are defined as (Green and Stevenson, 1986; Loague and Green, 1991)

$$E_{total} = \frac{(P_{total} - O_{total})}{O_{total}} \times 100 \quad (7)$$

$$E_{peak} = \frac{(P_{peak} - O_{peak})}{O_{peak}} \times 100 \quad (8)$$

$$\mathrm{RMSE} = \sqrt{\frac{1}{n}\sum_{i=1}^{n}(P_{\mathrm{i}} - O_{\mathrm{i}})^2} \times \frac{100}{\overline{O}} \tag{9}$$

where P_{total} and O_{total} are total predicted and observed values; P_{peak} and O_{peak} are peak predicted and observed values, P_{i} and O_{i} are predicted and observed instantaneous values and $\overline{O}$ is the mean of the observed data.

Following optimization of λ, β and k, the resulting model parameterization is validated by comparing predicted values of S_{t} and sediment concentration (C_{t}) with data observed during two suites of rainfall simulation experiments: (i) ROAD experiments 3, 6 and 8 (i.e. those not used in model calibration/optimization), and (ii) the eight WET experiments (median of eight events). The former are referred to as ROAD3, ROAD6 and ROAD8, and the latter as WET. Values of d_{n} for these ROAD experiments are 1·62, 1·56, 1·33 and 0·21 kg m^{-2} respectively (from Ziegler *et al.*, 2001a).

RESULTS

Optimization of the disturbance model yielded values of 44, 0·000025 and 1·42 for k, λ and β, respectively. Figure 4 shows the resulting prediction of ROAD12457 and HILL S_{t} and C_{t} using the optimized parameter set (results from this modelling method are referred to hereafter as KINEROS2 DE). The thin line is the DE simulation prediction from the prior work using the step function (KINEROS2 DE prior). Corresponding error and performance statistics are listed in Tables I and II. In Figure 5, the predictions of the S_{t} and C_{t} times-series for the ROAD 3, 6 and 8 validation events by the new KINEROS2 DE method (thick line) is compared with those by the prior method (thin line). The KINEROS2 DE S_{t} time-series prediction for the WET simulations is shown in Figure 6; note the step-function method was not validated with the WET data in the prior work. Prediction errors and performance values for all validation simulations are listed in Tables III and IV. Discharge values for all events are the same as those shown in the prior work (Ziegler *et al.*, 2001a).

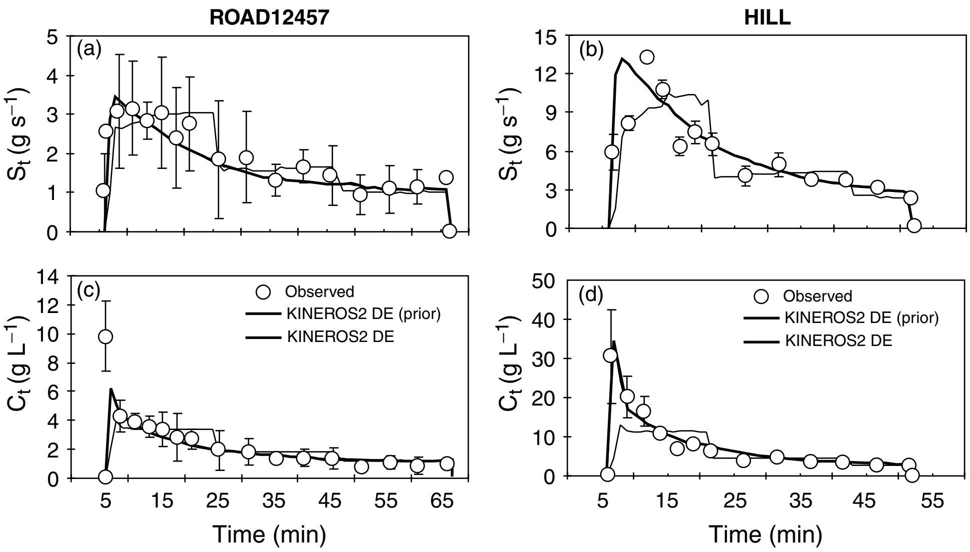

Figure 4. Post-calibration comparison of step function methodology used in a prior work (KINEROS2 DE (prior); Ziegler *et al.*, in 2001a) with the improved dynamic erodibility methodology (KINEROS2 DE) represented by Equation (6). Observed sediment transport (S_{t}) and concentration (C_{t}) values (circles) are medians of the experiments indicated in the title (i.e., ROAD12457 refers to ROAD rainfall simulation events, 1, 2, 4, 5 and 7; HILL is the median of four events); error bars are ± one median absolute deviation about the median

Table II. Model calibration results, including errors and performance statistics, for KINEROS2-predicted sediment concentration using the standard model approach (STD), the prior dynamic erodibility method (DE prior) and the technique introduced in this study (DE)

Simulation identity	Observed ($kg\ m^{-3}$)	Predicted ($kg\ m^{-3}$)	E_{total}[a] (%)	E_{peak} (%)	RMSE (%)
ROAD12457 STD	16·7	20·1	21	−78	105
ROAD12457 DE (prior)	16·7	20·9	25	−65	97
ROAD12457 DE	16·7	19·1	14	−39	40
HILL STD	55·9	44·9	−20	−84	116
HILL DE (prior)	55·9	61·7	10	−62	103
HILL DE	55·9	69·4	24	13	22

[a] E_{total} is error in total output estimate; E_{peak} is error in peak estimate; RMSE is root mean square error.

DISCUSSION

As shown in Figure 4, the new KINEROS2 DE method provides a more realistic estimate of the continuous sediment transport response than did the step function in the prior work. For both calibration simulations, ROAD12457 and HILL, substantial improvements are made in the estimation of the sediment output peaks and in simulation of the continuous time-series, as indicated by reduced values of E_{peak} and RMSE (Table I). Additionally, HILL E_{total} is improved, and the total error for ROAD12457 is still $\leq$5% (Table I). Despite having a more realistic response in the S_t time-series, peak output is substantially underpredicted by the new method for all validation events, as was the case using the step function in the prior method (Figure 5 and Table III). Underprediction may result, in part, from optimizing the parameters in Equation (6) with data from only two sediment depth scenarios. Additionally, on the small-scale rainfall simulation plots, sediment output peaks can be accentuated when loose material is stored near the plot outlet or within well-defined flow channels (i.e. ruts) where it can be flushed immediately, even by relatively small discharge volumes. In such cases, e.g. ROAD3 and ROAD6, a disproportionate percentage of the total loose sediment layer is removed during the initial sediment flush, as compared with the ROAD12457 or HILL experiments. Additionally, variations in microtopography between road sections having similar baseline erodibility values and loose surface material volumes could, therefore, produce substantial differences in S_t response. With respect to concentration, Figure 5 similarly shows that the new method generally simulates realistically the C_t times-series, except during the initial sediment flush peak. The relatively poor RMSE values for the ROAD6 and ROAD8 C_t predictions (Table IV) are exaggerated by the inability to simulate the initial sediment flush.

The WET simulation demonstrates the ability of the new DE method to predict the boundary condition of little or no loose surface sediment (Figure 6 and Tables III and IV). With a sediment availability parameter d_n of only 0·21 $kg\ m^{-2}$, the sediment output rate for this situation is controlled predominantly by the baseline erosion rate of the compacted road surface. Because availability of loose surface material is negligible, observed and modelled sediment output are nearly constant during these short events of constant rainfall intensity. Without the difficulty of simulating an initial sediment flush, model prediction for this condition is the best of all validation events.

CONCLUSIONS

By implementing an exponential decay disturbance model, the new dynamic erodibility modelling method produces a realistic prediction of the continuous sediment transport times-series for small-scale plots on unpaved roads. Difficulty in estimating peak sediment outputs during validation indicates that the optimized parameter set may have benefited from calibrating with rainfall simulation data from plots having a greater

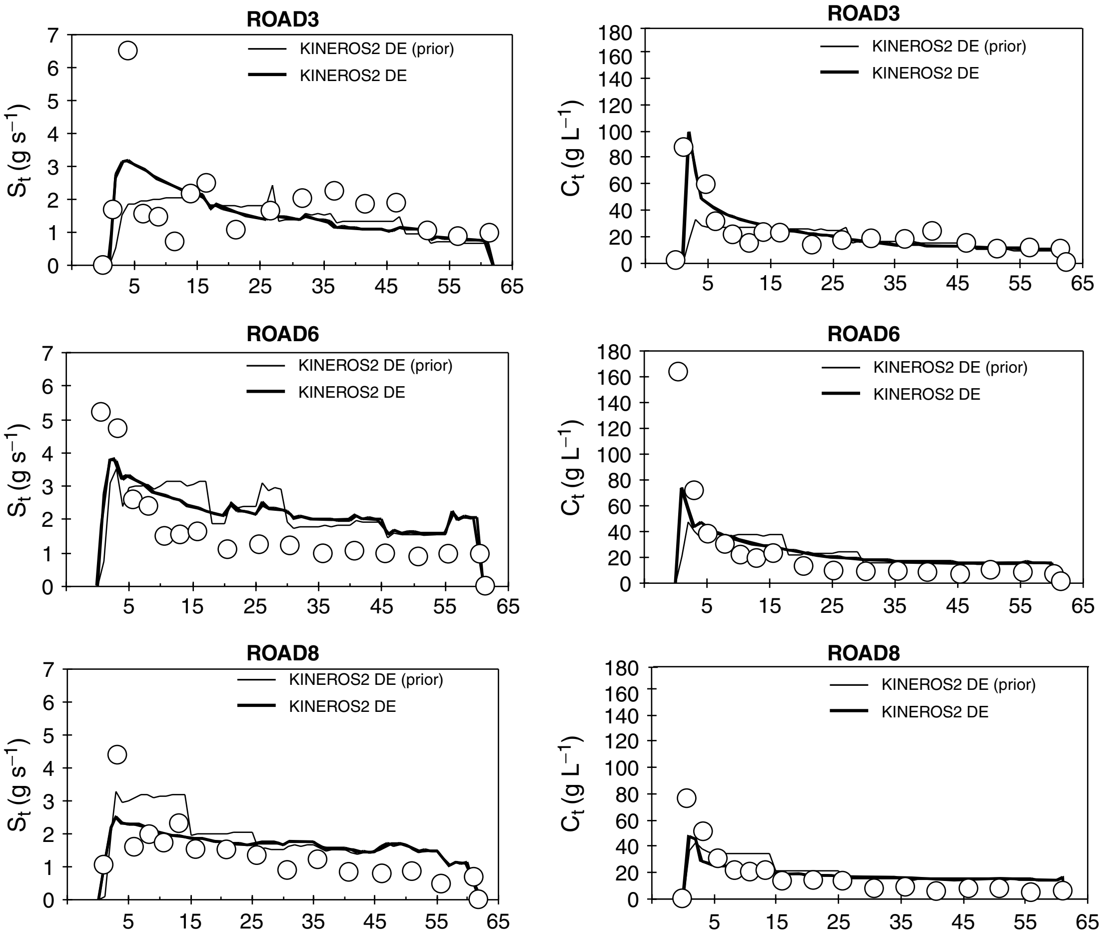

Figure 5. Validation results for the new dynamic erodibility method introduced herein (KINEROS2 DE) for ROAD rainfall simulation events 3, 6 and 8. The thin line represents the step function method used in a prior modelling effort (KINEROS2 DE (prior); Ziegler *et al*., 2001a). Circles are median values of observed sediment transport (S_t) and concentration (C_t) during the field rainfall simulations

range of pre-storm sediment availability than were used herein. Although the new DE method produces reasonable results for small-scale road plots, applicability to the PKEW road sections—where delayed runoff response and greater flow velocity/discharge will likely alter the fundamental sediment transport response that we observed on the simulation plots—will be more difficult. Further validation of the modelling method at the hillslope scale during natural events is needed before a final assessment can be made of its usefulness for simulating basin-wide road erosion in the study area (work in progress). Finally, it is still unclear to what extent small-scale road features, which affect process-based sediment transport (e.g. ruts), can be included in the model representation of a road surface.

ACKNOWLEDGEMENTS

Carl Unkrich, Southwest Watershed Research Center, USDA–ARS, Tuscon, AZ (help with KINEROS2); Randy Foltz, USDA Forest Service, Rocky Mountain Research Station, Moscow, ID (suggestions for the modelling approach); M.A. Nullet (engineering prowess); and T.T. Vana, UHM (help with the rainfall

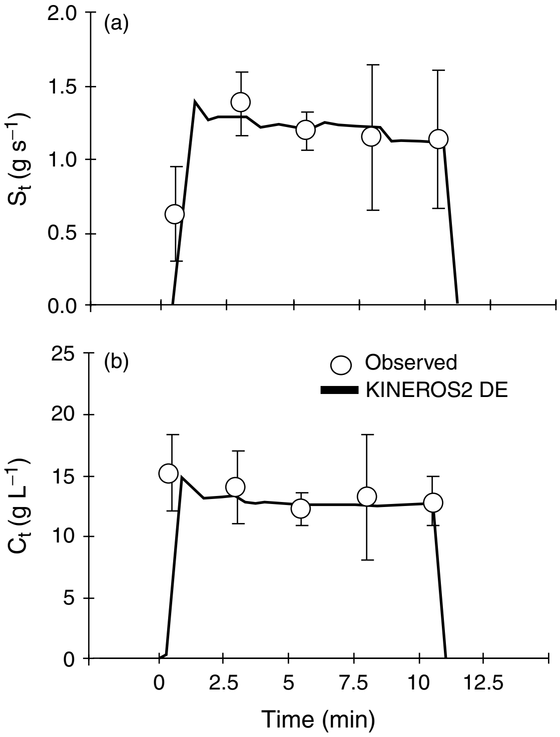

Figure 6. Prediction of observed sediment transport (S_t) and concentration (C_t) during the WET validation simulation using the dynamic erodibility method presented herein (Equation 6). Observed data (circles) are medians of the eight WET experiments; error bars are ± one median absolute deviation about the median

Table III. Model validation results, including errors and performance statistics, for KINEROS2-predicted sediment output using the standard model approach (STD), the dynamic erodibility method in the prior study (DE prior) and the technique introduced in this study (DE)

Simulation identity	Observed (kg)	Predicted (kg)	E_{total}[a] (%)	E_{peak} (%)	RMSE (%)
ROAD3 STD	5·6	5·0	−12	−68	76
ROAD3 DE (prior)	5·6	5·2	−7	−61	71
ROAD3 DE	5·6	5·2	−8	−58	64
ROAD6 STD	5·4	9·8	82	−26	118
ROAD6 DE (prior)	5·4	8·1	50	−40	92
ROAD6 DE	5·4	7·6	41	−38	65
ROAD8 STD	12·1	26·1	115	−72	84
ROAD8 DE (prior)	12·1	20·1	66	−63	63
ROAD8 DE	4·6	6·6	43	−38	53
WET STD	0·7	1·3	73	56	84
WET DE (prior)	NA	NA	NA	NA	NA
WET DE	0·7	0·7	0	−10	14

[a] E_{total} is error in total output estimate; E_{peak} is error in peak estimate; RMSE is root mean square error.

Table IV. Model validation results, including errors and performance statistics, for KINEROS2-predicted sediment concentration using the standard model approach (STD), the dynamic erodibility method in the prior study (DE prior) and the technique introduced in this study (DE)

Simulation identity	Observed (kg m^{-3})	Predicted (kg m^{-3})	E_{total}[a] (%)	E_{peak} (%)	RMSE (%)
ROAD3 STD	19·7	18·0	−8	−78	119
ROAD3 DE (prior)	19·7	19·0	−3	−67	113
ROAD3 DE	19·7	18·7	−5	−5	29
ROAD6 STD	14·3	28·1	96	−83	155
ROAD6 DE (prior)	14·3	23·0	61	−77	141
ROAD6 DE	14·3	21·7	52	−64	109
ROAD8 STD	12·1	26·1	115	−72	84
ROAD8 DE (prior)	12·1	20·1	66	−63	63
ROAD8 DE	12·1	19·4	60	−15	47
WET STD	14·8	22·3	50	52	88
WET DE (prior)	NA	NA	NA	NA	NA
WET DE	14·8	12·9	−13	−12	50

[a] E_{total} is error in total output estimate; E_{peak} is error in peak estimate; RMSE is root mean square error.

simulations). This project was partially funded by the National Science Foundation (grant nos. 9614259 and EAR0000546). Alan Ziegler was supported by an Environmental Protection Agency STAR Fellowship and a Horton Hydrology Research Award (Hydrological Section, American Geophysical Union).

REFERENCES

Green IRA, Stephenson D. 1986. Criteria for comparison of single event models. *Hydrological Sciences Journal* **31**: 395–411.

Loague K, Green RE. 1991. Statistical and graphical methods for evaluating solute transport models: overview and application. *Journal of Contaminant Hydrology* **7**: 51–73.

Megahan WF. 1974. *Erosion Over Time: a model*. USDA–Forest Service Research Paper Report INT-156. Intermountain Research Station: Ogden UT; 14 pp.

Schmidt-Vogt D. 1998. Defining degradation: the impacts of swidden on forests in northern Thailand. *Mountain Research and Development* **18**(2): 135–149.

Smith RE, Goodrich DC, Quinton JN. 1995. Dynamic, distributed simulation of watershed erosion: the KINEROS2 and EUROSEM models. *Journal of Soil and Water Conservation* **50**(5): 517–520.

Smith RE, Goodrich DC, Unkrich CL. 1999. Simulation of selected events on the Catsop catchment by KINEROS2 A report for the GCTE conference on catchment scale erosion models. *Catena* **37**: 457–475.

Ziegler AD, Giambelluca TW. 1997. Importance of rural roads as source areas for runoff in mountainous areas of northern Thailand. *Journal of Hydrology* **196**(1/4): 204–229.

Ziegler AD, Sutherland RA, Giambelluca TW. 2000a. Partitioning total erosion on unpaved roads into splash and hydraulic components: the roles of inter-storm surface preparation and dynamic erodibility. *Water Resources Research* **36**(9): 2787–2791.

Ziegler AD, Sutherland RA, Giambelluca TW. 2000b. Runoff generation and sediment transport on unpaved roads, paths, and agricultural land surfaces in northern Thailand. *Earth Surface Processes and Landforms* **25**(5): 519–534.

Ziegler AD, Giambelluca TW, Sutherland RA. 2001a. Erosion prediction on unpaved mountainous roads in northern Thailand: validation of dynamic erodibility modeling using KINEROS2. *Hydrological Processes* **15**: 337–358.

Ziegler AD, Sutherland RA, Giambelluca TW. 2001b. Interstorm surface preparation and sediment detachment by vehicle traffic on unpaved mountain roads. *Earth Surface Processes and Landforms* **26**(3): 235–250.

Ziegler AD, Sutherland RA, Giambelluca TW. 2001c. Acceleration of Horton overland flow and erosion by footpaths in an agricultural watershed in Northern Thailand. *Geomorphology* **1**(4): 249–262.

